Relativistic momentum space wave equations and meson spectroscopy

Alan J. Sommerer and John R. Spence
Department of Physics and Astronomy, Iowa State University, Ames, Iowa 50011

James P. Vary
Department of Physics and Astronomy, Iowa State University, Ames, Iowa 50011
and Institute for Theoretical Physics, University of Heidelberg, Heidelberg, Germany
(Received 26 July 1993)

We examine the applicability of a class of relativistic two-body equations, the quasipotential equations (QPE's), as a tool for investigating hadronic physics. We show that the QPE's traditionally used in nuclear physics may be viewed as special cases of a more general QPE written in terms of three parameters. The behavior of the QPE's is analyzed in terms of these parameters in the small, intermediate, and large coupling regimes, including fits to light and heavy meson spectra. A subset of QPE's is identified which provide fits to the heavy mesons with rms deviations from experiment of 32–36 MeV.

PACS number(s): 03.65.Pm, 11.10.St, 12.39.Pn

I. INTRODUCTION

The nearly two decades since the discovery of heavy $q\bar{q}$ bound states has seen a plethora of tools developed for the study of mesons as a window on hadronic physics. One would of course like to investigate hadronic properties and test quantum chromodynamics (QCD) by solving QCD directly. However, the non-Abelian nature of the theory and the consequent well-known complexities make solutions for nonperturbative calculations of realistic systems too difficult at present, and we must turn to other methods. The methodology that comes closest in spirit to a direct solution of QCD is lattice QCD computations [1]. Unfortunately, lattice QCD has difficulties of its own, both in the details of the computational techniques and in the limitations of computer resources. As a consequence, many alternative methods of examining hadron physics have arisen which retain connections to QCD in varying degrees.

Prominent among the examples of these methods have been the constituent quark potential models. Comparatively simple, nonrelativistic representatives of such models were naturally among the earliest tools employed in attempting to study the $c\bar{c}$ bound states as the "hydrogen atoms" of the hadrons [2]. Though these early models achieved some success in reproducing the general features of heavy quarkonia spectra, it was believed that the constituent quark models would break down when applied to the lighter mesons. In addition, the connection of the potential models to QCD was unclear.

More recently, though, a number of constituent quark potential models which include aspects of relativistic dynamics have proven able to describe both heavy and light meson properties with some success [3–5]. Moreover, evidence has become available from lattice calculations supporting a connection between the potential models and QCD [4–6].

Important among the relativistic extensions of the potential models have been those related to the Bethe-Salpeter wave equation treatment [7]. These Bethe-Salpeter-inspired techniques have the advantage of a link to the underlying field theory, and even after making approximations which are necessary to solve these equations, relativistic and nonperturbative aspects of the physics survive.

These appealing features have prompted several efforts in recent years to devise powerful methods of solution for these wave equations and to apply the formalism to the study of hadronic physics [8–10]. In this paper, we examine the applicability of a class of Bethe-Salpeter-related equations, the quasipotential equations, as a tool for investigating QCD bound states in the meson sector. These equations have been used successfully in describing relativistic aspects of nuclear physics in the past [11], and we will show that a subclass of these equations provides a powerful means of investigating hadronic physics as well.

The paper is arranged as follows. In the next section we introduce the Bethe-Salpeter equation (BSE) and the quasipotential equations (QPE's) that have been traditionally used in nuclear physics. Section III will present a comparison of solutions of various traditional QPE's in the small coupling regime. In Sec. IV we will show that the traditional QPE's may be considered to be special cases of a parametrized QPE which we introduce. We will show that by manipulation of the parameter values of this general equation, a new QPE may be constructed which better reproduces perturbative results at small coupling than the QPE's traditionally used. In Sec. V we use a set of QPE's to fit meson spectra, comparing the results of the various equations in terms of the parameters of the generalized QPE, and in Sec. VI we fit the light $q\bar{q}$ states with one of the QPE's. In Sec. VII we briefly examine the deep binding limits of the relativistic wave equations. We summarize in Sec. VIII.

II. RELATIVISTIC TWO-BODY WAVE EQUATIONS

The Bethe-Salpeter equation is, in principle, a complete nonperturbative description of the relativistic two-body problem governed by a quantum field theory. The BSE is an integral equation having a kernel determined from the amplitudes of the two-particle diagrams of all orders in the coupling which is integrated over the four-momenta of the internal two-body propagator. The BSE for a bound state may be written in the form

$$G^{-1}(P,p)\psi(P,p) = \int \frac{d^4p'}{(2\pi)^4} V(P,p-p')\psi(P,p'). \quad (1)$$

In this equation, P is the four-momentum of the bound state, p is the relative four-momentum of the constituents, V is the interaction kernel, and G is the two-particle propagator.

In practice, an approximation is made to the BSE by truncating its interaction kernel to some fixed order in the coupling. Typically, only the lowest order one-boson-exchange term in the interaction is kept in the kernel, resulting in what are called ladder equations. A common additional approximation is the reduction of Eq. (1) to three dimensions. Numerous methods for accomplishing the reduction to three dimensions have been proposed which involve fixing, in some way, the zeroth component of the relative momentum. An early such procedure is that of Salpeter [12] wherein the zeroth component of the relative momentum is set equal to zero in the kernel, resulting in the replacement $V(p-p') \to V(\mathbf{p}-\mathbf{p}')$. This replacement then allows analytic integration of the zeroth components of the momentum in the propagator, completing the reduction to three dimensions.

In this paper we will be concerned with QPE's, a class of relativistic wave equations which achieve reduction to three dimensions by specifying the relative energy dependence in a covariant way. With the definition $\chi = G^{-1}\psi$, we may rewrite Eq. (1) as

$$\chi = VG\chi. \quad (2)$$

The method of the quasipotential formalisms is to express this equation as the set of equations

$$\chi = Wg\chi\ , \quad (3a)$$

$$W = V + V(G-g)W. \quad (3b)$$

Here, g is a covariant propagator which reduces Eq. (3a) to three dimensions, and W is defined by the iterative equation (3b). Equations (3) are formally equivalent to Eq. (2). To achieve the simplifications associated with the ladder approximation, we approximate W by its zeroth iteration, $W \approx V$, so that a covariant three-dimensional ladder equation results,

$$\chi = Vg\chi. \quad (4)$$

Each of the quasipotential equations traditionally used in nuclear physics corresponds to a different choice of the function g. It has been shown that there are an infinite number of functions g which will produce a covariant three-dimensional equation in the form of Eq. (4) [13]. Of the possible functions g, we consider those corresponding to the Blankenbecler-Sugar equation [14], the Kadyshevsky equation [15], the Gross equation [16], the Thompson equations [17], the Todorov equation [18], and the Erkelenz-Holinde equation [19]. For spinless particles a covariant form for the function g is, specializing to the case of constituents of equal mass m,

$$g = 2\pi i \int_{4m^2}^{\infty} \frac{ds'}{s'-s-i\epsilon} f(s,s')\delta^+(\nu_1)\delta^+(\nu_2), \quad (5)$$

where in the center of mass frame $s = P^2$, $s' = P'^2$, and $f(s,s')$ is an arbitrary function satisfying

$$f(s,s) = 1. \quad (6)$$

This condition on f ensures that the resulting QPE maintains elastic unitarity and has the proper Lippmann-Schwinger equation as its nonrelativistic limit. The δ^+ functions are defined by $\delta(x^2-a^2) = \delta^+(x^2-a^2)+\delta^-(x^2-a^2)$ where $\delta^{\pm}(x^2-a^2) = \frac{1}{2a}\delta(x \mp a)$. The reduction to three dimensions is performed by using the delta functions in Eq. (5) to specify the relative energy of the interaction. For some QPE's, this is done by restricting one of the particles to its mass shell which leaves a nonzero relative energy dependence in the interaction. To accomplish this, the arguments of the delta functions are chosen to be

$$\nu_1 = (\tfrac{1}{2}P + p')^2 - m^2 \quad (7a)$$

and

$$\nu_2 = (P' - \tfrac{1}{2}P - p')^2 - m^2. \quad (7b)$$

For other QPE's the two particles are specified to be equally off their mass shell leaving no relative energy dependence. For these QPE's,

$$\nu_1 = (\tfrac{1}{2}P' + p')^2 - m^2 \quad (8a)$$

and

$$\nu_2 = (\tfrac{1}{2}P' - p')^2 - m^2. \quad (8b)$$

The integration of Eq. (6) is carried out using one of the delta functions, and the remaining delta function reduces the QPE to a three-dimensional equation.

The functions $f(s,s')$ utilized by each of the traditional QPE's we study are listed in Table I along with the f for a new equation to be introduced in the following section. Also indicated in the table is the relative energy dependence characterizing each equation.

For the case of fermion constituents, there is an additional freedom in the choice of the matrix structure of g. In this paper, we adopt the method of Ref. [11] where the function g is written

$$g = 2\pi i \int_{4m^2}^{\infty} \frac{ds'}{s' - s - i\epsilon} f(s', s)\delta^{(+)}(\nu_1)\delta^{(+)}(\nu_2)(\tfrac{1}{2}\not{P}' + \not{p}' - m)(\tfrac{1}{2}\not{P}' - \not{p}' - m) \tag{9}$$

when the delta function arguments are those of Eq. (8). For the delta function arguments given in Eq. (7),

$$g = 2\pi i \int_{4m^2}^{\infty} \frac{ds'}{s' - s - i\epsilon} f(s', s)\delta^{(+)}(\nu_1)\delta^{(+)}(\nu_2)(\tfrac{1}{2}\not{P} + \not{p}' - m)(\not{P}' - \tfrac{1}{2}\not{P} - \not{p}' - m). \tag{10}$$

This treatment results in the appearance of positive energy projection operators in the functions g, so that the QPE's retain only positive energy components of their amplitudes.

This variety of three-dimensional relativistic wave equations has inspired several attempts to compare and contrast them in an effort to determine which among them is the "best" equation to use. Different criteria have been used in comparing the various equations. Woloshyn and Jackson [20] examined several three-dimensional scattering equations for spinless "nucleons" by comparing the first iteration of their kernels at threshold with the analogous term from the four-dimensional BSE. Gross [21] has made another comparison of various three-dimensional equations by examining their limiting behavior as one of the particle masses is taken to infinity. A study by Silvestre-Brac and co-workers [22] compared the small coupling bound state energy predictions of several spin-0–spin-0 equations with the predictions of the Schrödinger equation. The differing behavior of the equations at larger coupling was also noted. Cooper and Jennings [23] have examined a variety of equations based on their ability to reproduce the correct one-body limit when one of the particle masses tends to infinity. The conclusions reached regarding the suitability of a given QPE depended on the criteria applied in these various works.

In this paper, we will introduce a generalized QPE written in terms of three parameters, two of which are independent. Each of the QPE's mentioned above will correspond to a particular choice of parameters of the generalized equation. The behavior of the generalized QPE, and hence of the standard QPE's we study, will be examined in terms of the parameters. Once the behavior of the equation in terms of the parameters is understood, the parameters may be adjusted to construct a QPE that optimally satisfies some specified criterion. In particular, one of our goals will be to identify those parameter values which yield QPE's that best describe QCD observables. In the present investigation, these observables will be meson masses.

We will analyze bound states of fermion-antifermion pairs. We will compare the energy predictions of the standard QPE's at both the low coupling typical of QED and at the larger couplings typical of QCD. At low coupling we compare the QPE solutions to the predictions of perturbation theory. For larger couplings, we will compare the quality of the various QPE's fits to the heavy meson spectrum as a test of their utility.

TABLE I. The functions $f(s', s)$ used in the replacement propagator g for each of the QPE's. If the QPE restricts one of the particles to its mass shell, a "yes" appears in the last column. A "no" indicates the QPE places the particles equally off shell so that there is no relative energy dependence. The New and New+retardation equations are the $a = +1$ equations of Sec. IV.

QPE	$f(s', s)$	Relative energy dependence?
Blankenbecler-Sugar	1	no
Erkelenz-Holinde	1	yes
Todorov	$\sqrt{s'}/\sqrt{s}$	no
Thompson I	$(\sqrt{s} + \sqrt{s'})/2\sqrt{s'}$	no
Kadyshevsky	$(\sqrt{s} + \sqrt{s'})/2\sqrt{s'}$	yes
Thompson II	$(\sqrt{s} + \sqrt{s'})/2\sqrt{s}$	no
Gross	$(\sqrt{s} + \sqrt{s'})/2\sqrt{s}$	yes
New	$\sqrt{s}/\sqrt{s'}$	no
New+retardation	$\sqrt{s}/\sqrt{s'}$	yes

III. COMPARISON OF THE QPE'S AT SMALL COUPLING

The fourth order perturbative prediction for the binding energy B of a ground state pseudoscalar fermion-antifermion pair is (in units of the fermion mass) [24]

$$B = -\frac{1}{4}\alpha^2 - \frac{21}{64}\alpha^4 \simeq -\frac{1}{4}\alpha^2 - 0.328\alpha^4, \tag{11}$$

where α is the coupling strength. Reference [24] obtains this result from within a momentum space Bethe-Salpeter treatment where the instantaneous component of the photon propagator in Feynman gauge is used to construct the coupled spinor Salpeter's equations. The corrections to the instantaneous result are handled perturbatively, also by a treatment due to Salpeter [12]. Equation (5) may be obtained in other ways. Reference [25], for example, derives this expression from within a Hamiltonian formulation in coordinate space.

We have performed an evaluation of the standard ladder QPE's for this system based on their ability to phenomenologically reproduce this perturbative result in the small coupling regime. We employ a B-spline Galerkin method of solving the integral equations which has been described elsewhere [10,26], but we will give a brief overview of the technique in the Appendix.

Taking the fermion mass to be unity, we first solved each of the traditional (ladder) QPE's as a function of the coupling strength, letting the coupling vary from 0 to 0.012, a range that straddles the fine structure constant. We subtracted the second order quantity $-\alpha^2/4$ from all of the results and fit the residual to a curve of the form

TABLE II. Solutions of the QPE's as a function of coupling strength α were fit to a curve of the form $-0.25\alpha^2 - k\alpha^4$. The coefficient of the fourth order term k given by each of the QPE's is shown in the second column and is to be compared with the value 0.328 predicted by perturbation theory. The last two columns show the values of the parameters of the generalized $f(s', s)$ corresponding to the QPE's. The New and New+retardation equations are the $a = +1$ equations of Sec. IV. The first five QPE's listed have no relative energy dependence (no retardation) in their interactions. The last four QPE's (those listed below the dashed line) have relative energy dependence (retardation) in their interactions.

QPE	Fourth order coefficient k	a	c
New	0.323	1	0
Thompson I	0.450	0	1
Blankenbecler-Sugar	0.576	0	0
Thompson II	0.705	−1	1
Todorov	0.834	−1	0
New+retardation	0.453	1	0
Kadyshevsky	0.581	0	1
Erkelenz-Holinde	0.711	0	0
Gross	0.852	−1	1

$-k\alpha^4$. We also did a fit to a curve of the form $k_1\alpha^3 + k_2\alpha^4$, but in all cases the coefficient of the α^3 term was small enough to justify comparing only the fourth order coefficients. The QPE's were then ranked according to how closely the coefficient of the fourth order fit matched the fourth order coefficient 0.328 predicted by perturbation theory. The results are presented in the first two columns of Table II. The two rightmost columns of the table and the "New" and "New+retardation" equations appearing in the list will be explained in the next section. Note that all the QPE's, with the exception of the "New" equation, show more binding than that predicted by perturbation theory.

The fourth order contributions to binding energy as given in Table II for each of these QPE's are plotted against the coupling strength in Fig. 1. Figure 1 shows that, at such small coupling, the differences in binding energy predicted by each of the QPE's are of the order of parts per 10^9. It is also clear from the figure that the differences between the various equations become more pronounced with increasing coupling. How significant are these differences at large coupling? One answer is given when we apply these QPE's to fit the heavy meson spectrum. Before that, however, in the next section we introduce a generalized QPE in three parameters that will allow us to understand the different behavior of the standard equations as given in Table I, and to construct a new QPE that better satisfies the perturbative criterion of Eq. (11).

IV. GENERALIZED QPE

All of the functions $f(s', s)$ employed by the QPE's listed in Table I may be written in the form

$$f(s', s) = \sqrt{s^a}\sqrt{s'^b}\left(\frac{\sqrt{s} + \sqrt{s'}}{2}\right)^c. \tag{12}$$

The condition of Eq. (6) is then equivalent to the condition

$$a + b + c = 0. \tag{13}$$

This condition implies that only two of the parameters a, b, and c are independent, and in the rightmost columns of Table II we show the values of the parameters a and c corresponding to the various QPE's.

The three-dimensional propagator of the QPE which arises from Eq. (12) will be proportional to

$$g(a, c) = \frac{E^a(E + 2\omega)^c}{2^{c-b}\omega^{1-b}(4\omega^2 - E^2)}, \tag{14}$$

where $\omega = \sqrt{\mathbf{p}^2 + m^2}$, and from (13), b is understood to be equal to $-a - c$. For the case $c = 0$,

$$g(a, 0) = \frac{E^a}{2^a\omega^{a+1}(4\omega^2 - E^2)}. \tag{15}$$

For the case $c = 1$, Eq. (14) becomes

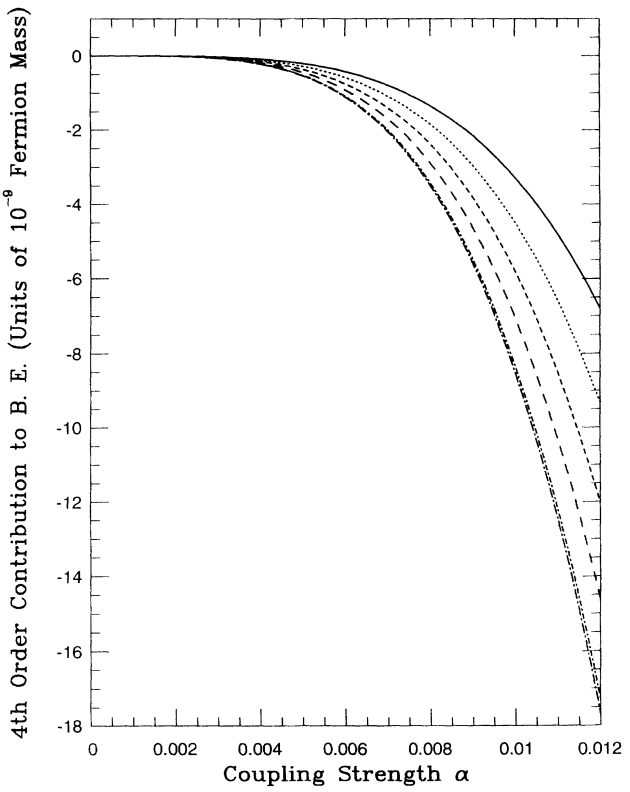

FIG. 1. Plots of the fourth order term in the QPE solution fits (see Table II) in units of 10^{-9} times the fermion mass compared with a plot of fourth order perturbative contribution to the binding energy for fermion mass equal to unity. From top to bottom: Solid curve: fourth order perturbative contribution to binding energy ($-0.328\alpha^4$); dotted curve: Thompson I and New+retardation ($-0.45\alpha^4$); short dashed curve: Blankenbecler-Sugar and Kadyshevsky ($-0.58\alpha^4$); long dashed curve: Thompson II and Erkelenz-Holinde ($-0.71\alpha^4$); short dash-dotted curve: Todorov ($-0.83\alpha^4$); long dash-dotted curve: Gross ($-0.85\alpha^4$). The curve produced by the New equation (with no retardation) of Sec. IV lies essentially on top of the solid curve.

$$g(a,1) = \frac{E^a}{(2\omega)^{a+2}(2\omega - E)}. \tag{16}$$

In the nonrelativistic limit, the propagators (15) and (16) reduce to $[4m(mB + p^2)]^{-1}$, where B is the binding energy, for any value of a. At large momentum, however, these propagators behave differently with respect to momentum and energy depending on the value of the parameter a.

These differences may be emphasized by writing the propagators in their large momentum ($p \gg m$) limits. In this limit, the $c = 0$ propagator (15) becomes

$$g(a,0) \to \frac{E^a}{2^{a+2}p^{a+3}}, \tag{17}$$

and the $c = 1$ propagator (16) becomes

$$g(a,1) \to \frac{E^a}{(2p)^{a+3}}. \tag{18}$$

The more negative the parameter a is, the larger the propagators are at high momentum. The more positive a is, the smaller the propagators are at high momentum.

For example, with $a = -1$, the propagators behave as $1/(Ep^2)$ at large momentum. As a bound state is made more relativistic and more tightly bound by increasing the coupling of the interaction, the energy of the state falls further and further below $2m$. Since the energy appears in the denominator of the propagator for $a = -1$, this means the propagator is enhanced for more deeply bound states. Additionally, the $a = -1$ propagator falls off as only p^{-2} for large momentum.

For $a = +1$, as an example of a positive a propagator, the large momentum behavior is E/p^4. For deeply bound, relativistic states, such a propagator will be diminished because it is proportional to the energy of the state, rather than inversely proportional as for the $a < 0$ case. In addition, the $a = 1$ propagator falls off as p^{-4} at high momentum.

For those propagators with the same value of a, the $c = 1$ propagator will be smaller by a factor of 2 than the $c = 0$ propagator at high momentum.

In the QPE's, the propagator g multiplies the interaction kernel. In general, as the size of the propagator increases, the binding energy increases. These effects will be most important for relativistic systems. They are small but already apparent in the low coupling regime, however.

We expect that the effect of the propagator will be largest (smallest), and hence the binding energy greatest (least), for those QPE's having propagators with negative (zero or positive) a, and this is confirmed by Table II. Those equations corresponding to $a = -1$ predict more binding energy than those corresponding to $a = 0$. Among those equations having the same value of a, those equations having $c = 0$ show slightly more binding than those with $c = 1$. In addition, Table II shows that those equations having relative energy dependence (retardation) in their interactions predict more binding energy than the analogous equation with no relative energy dependence.

Table II indicates that all the traditional QPE's we study predict more binding energy than fourth order perturbation theory. We easily construct a QPE that brings improved agreement with the perturbation results by adjusting the parameters of the generalized propagator. As explained above, increasing the positive value of the parameter a will decrease the binding energy predicted by the QPE. We may therefore "tune" the propagator by adjusting the value of a upwards until a match with perturbation theory is achieved. The best fit is obtained with a value for a very slightly less than unity. Performing a fourth order fit as described above on a QPE with the parameters $a = 1$ and $c = 0$ (and with no relative energy dependence) yields the result $B = -\frac{1}{4}\alpha^2 - 0.323\alpha^4$, very close to the fourth order perturbation prediction. For convenience, we refer to the QPE with $a = 1$, $c = 0$ and no retardation as "New" in the tables and figure captions. The QPE with $a = 1$, $c = 0$ and *with* relative energy dependence, referred to as "New+retardation" in Tables I and II, yields the result $B = -\frac{1}{4}\alpha^2 - 0.453\alpha^4$ in a fourth order fit.

V. INTERMEDIATE COUPLING REGIME: MESON SPECTRUM FITS

In this section, we will be concerned with reproducing the spectrum of experimentally known charmonium and bottomonium states. Because we are chiefly interested in the relative behaviors of the QPE's as a function of the parameters of the generalized propagator, Eq. (14), in these fits we will use only those equations having zero relative energy, i.e., all those equation listed above the dashed line in Table II. These equations cover a wider range of parameter values than those QPE's listed below the dashed line, and they come closer to reproducing the perturbative energy predictions for small coupling than the corresponding QPE's which use relative energy dependence.

In the fits we used a one-gluon-exchange interaction $V_{\rm OGE}$ and a long range linear confining potential $V_{\rm con}$. Specifically, in momentum space these take the form

$$V_{\rm OGE} = -\frac{4}{3}\alpha_s \frac{\gamma_\mu^a \gamma_\mu^b}{(\mathbf{p} - \mathbf{p}')^2}, \tag{19}$$

which results from setting the relative energy equal to zero from within the Feynman gauge, and

$$V_{\rm con} = \sigma \lim_{\mu \to 0} \left(\frac{\partial}{\partial \mu}\right)^2 \frac{\Gamma^a \Gamma^b}{-(\mathbf{p} - \mathbf{p}')^2 + \mu^2}. \tag{20}$$

α_s is the strong coupling which is weighted by the $q\bar{q}$ color factor of $\frac{4}{3}$, and σ is the string tension, the strength of confining part of the interaction. The matrices $\Gamma^a\Gamma^b$ represent the freedom of choice for the Lorentz structure of $V_{\rm con}$ which may be scalar, pseudoscalar, vector, or combinations of these. The form of the confining interaction used here, along with the cubic B-spline Galerkin method of solving the integral equations, allows for the use of a linear confining potential in a momentum space equation. We give a brief outline of the Galerkin method of solution

in the Appendix. More complete details of our solution method may be found in Refs. [8,10,26].

In the nonrelativistic limit, these interactions correspond to the coordinate space potential

$$V(r) = -\frac{4}{3}\frac{\alpha_s}{r} + \sigma r. \quad (21)$$

We do not find a need for a constant term which is often utilized in other efforts [5,9]. Lattice results support the selection of a linear confining potential which is predominantly scalar [6].

We list in Table III the 12 $c\bar{c}$ and 12 $b\bar{b}$ experimentally known states. The masses given for each state (except the h_c) are the averages given by the Particle Data Group [27]. The spectrum of the 24 states of Table III was fit using the four traditional QPE's of Table I having no relative energy dependence, as well as the $a = 1$, $c = 0$ new equation with no retardation introduced in the previous section. The fits were performed by adjusting four quantities: the gluon coupling α_s, the string tension σ of the confining potential, and the charm and bottom quark constituent masses.

We list in Table IV the spectra produced by the various QPE's with scalar linear confinement. We performed the fits by minimizing the rms deviation between the masses predicted by the QPE's and the experimental masses. The masses predicted by the QPE's were matched with the mesons according to the spectral conjectures listed in the first column of Table III. The most ambiguous assignment was for the $\psi(4415)$ meson. Both the $4\,^3S_1$ and $3\,^3D_1$ states of charmonium have masses near 4415 MeV according to each of the QPE's. Interpreting the $\psi(4415)$ meson as the fourth S state instead of the third D state degraded the rms deviation of each of the fits by 2 or 3 MeV.

TABLE III. Charmonium and bottomonium states with measured masses in MeV. An asterisk indicates the state is not known experimentally. The spectral assignments for each state given in the first column are conjectures based on theoretical fits to the spectrum.

$N\,^{2S+1}L_J$	$c\bar{c}$ name	$c\bar{c}$ mass	$b\bar{b}$ name	$b\bar{b}$ mass
$1\,^1S_0$	$\eta_c(1S)$	2979	$\eta_b(1S)$	*
$2\,^1S_0$	$\eta_c(2S)$	3594	$\eta_b(2S)$	*
$1\,^3S_1$	$J/\psi(1S)$	3097	$\Upsilon(1S)$	9460
$2\,^3S_1$	$\psi(2S)$	3686	$\Upsilon(2S)$	10023
$3\,^3S_1$	$\psi(4040)$	4040	$\Upsilon(3S)$	10355
$4\,^3S_1$	$\psi(4S)$	*	$\Upsilon(4S)$	10580
$5\,^3S_1$	$\psi(5S)$	*	$\Upsilon(10860)$	10865
$6\,^3S_1$	$\psi(6S)$	*	$\Upsilon(11020)$	11019
$1\,^3P_0$	$\chi_{c0}(1P)$	3415	$\chi_{b0}(1P)$	9860
$2\,^3P_0$	$\chi_{c0}(2P)$	*	$\chi_{b0}(2P)$	10232
$1\,^1P_1$	$h_c(1P)$	3526	$h_b(1P)$	*
$1\,^3P_1$	$\chi_{c1}(1P)$	3511	$\chi_{b1}(1P)$	9892
$2\,^3P_1$	$\chi_{c1}(2P)$	*	$\chi_{b1}(2P)$	10255
$1\,^3P_2$	$\chi_{c2}(1P)$	3556	$\chi_{b2}(1P)$	9913
$2\,^3P_2$	$\chi_{c2}(2P)$	*	$\chi_{b2}(2P)$	10268
$1\,^3D_1$	$\psi(3770)$	3770	$\Upsilon_1(1D)$	*
$2\,^3D_1$	$\psi(4160)$	4159	$\Upsilon_1(2D)$	*
$3\,^3D_1$	$\psi(4415)$	4415	$\Upsilon_1(3D)$	*

We also performed fits using linear confining potentials having vector Lorentz structure. We list the results of these fits in Table V.

Tables IV and V show that we can divide the QPE's into two groups according to the quality of their heavy meson fits. The first group consists of those equations which correspond to $a \geq 0$ in terms of the parametrized propagator, Eq. (14). These equations are the Blankenbecler-Sugar, Thompson I, and the new QPE. The fits produced by each of these QPE's have rms deviations in the range 32–36 MeV for the case of the scalar confinement potential. The second group consists of the other two QPE's, which correspond to $a = -1$ in the parametrized propagator, and their fits are of lesser quality. The differences between the quality of the fits with these two groups is not as pronounced in the vector linear confinement case.

The best fits with the vector confinement are less competitive than those using the scalar confinement for the three QPE's giving the best fits above. Because the best

TABLE IV. Charmonium and bottomonium spectra produced by the best fits for various QPE's. Interactions were ladder gluon exchange and scalar linear confinement potential. All meson masses are in MeV. Blankenbecler-Sugar results are in column BS, Thompson I and II results under Th I and Th II, Todorov equation results under T, and the $a = 1$, $c = 0$ equation with no retardation introduced in Sec. IV under New. At the bottom are listed the rms deviation from experiment for each fit and the "best-fit" values of the parameters.

Meson	m_{expt}	BS	Th I	Th II	T	New
$\eta_c(1S)$	2979	2981	3017	3173	3198	3048
$\eta_c(2S)$	3595	3584	3610	3661	3655	3631
$\chi_{c0}(1P)$	3415	3426	3403	3519	3533	3395
$\chi_{c1}(1P)$	3511	3523	3497	3501	3513	3475
$h_c(1P)$	3526	3525	3506	3479	3491	3488
$J/\psi(1S)$	3097	3174	3148	3183	3203	3136
$\psi(2S)$	3686	3688	3681	3668	3659	3678
$\psi(3770)$	3770	3778	3758	3739	3741	3737
$\psi(4040)$	4040	4033	4052	3995	3959	4066
$\psi(4160)$	4159	4091	4100	4039	4011	4102
$\psi(4415)$	4415	4345	4381	4283	4229	4404
$\chi_{c2}(1P)$	3556	3601	3594	3526	3535	3582
$\chi_{b0}(1P)$	9860	9823	9826	9816	9809	9828
$\chi_{b0}(2P)$	10232	10190	10191	10207	10210	10195
$\chi_{b1}(1P)$	9892	9867	9879	9814	9805	9881
$\chi_{b1}(2P)$	10255	10232	10236	10205	10207	10235
$\Upsilon(1S)$	9460	9467	9451	9517	9499	9444
$\Upsilon(2S)$	10023	9991	9992	9995	9993	9995
$\Upsilon(3S)$	10355	10340	10337	10355	10359	10336
$\Upsilon(4S)$	10580	10622	10614	10655	10661	10610
$\Upsilon(10860)$	10865	10866	10855	10917	10921	10850
$\Upsilon(11020)$	11019	11085	11072	11152	11153	11066
$\chi_{b2}(1P)$	9913	9944	9965	9861	9852	9973
$\chi_{b2}(2P)$	10268	10296	10305	10250	10251	10306
rms (MeV)	——	36	32	77	89	35
α_s	——	0.253	0.319	0.035	0.015	0.374
σ (GeV^2)	——	0.251	0.212	0.370	0.437	0.188
m_c (GeV)	——	1.37	1.41	1.20	1.19	1.44
m_b (GeV)	——	4.67	4.74	4.44	4.39	4.79

fits were produced with the scalar form of the confinement, and because confinement is expected to be largely scalar in nature from lattice computations, we will restrict the following discussion to the fits with the scalar confinement potential.

The fitted value of the gluon coupling was controlled largely by the S states which have large probability density at the origin in coordinate space where the Coulomb-like potential is the strongest. The $a = 1$ new equation, which has the weakest propagator at large momentum, required the strongest gluon coupling. The two $a = 0$ equations produced fits with lower gluon coupling. However, the two $a = -1$ equations, having the largest propagators at high momentum, required very weak couplings to obtain reasonable S states. These $a = -1$ equations drag the S-state energies down at a coupling strength too small to give a competitive fit for the P and D states.

The value of the string tension for each equation was determined largely by the P and D states which have most of their probability density in the long range linear part of the potential. The high momentum behavior of the equations is less important for these states, and, consequently, the string tensions produced by the various equations are much closer to each other than are the gluon couplings.

Those equations giving the largest gluon coupling gave the largest quark masses and the smallest string tension, and vice versa.

TABLE V. Charmonium and bottomonium spectra produced by the best fits for various QPE's. Interactions were ladder gluon exchange and vector linear confinement potential. All meson masses are in MeV. Blankenbecler-Sugar results are in column BS, Thompson I and II results under Th I and Th II, Todorov equation results under T, and the $a = 1$, $c = 0$ equation with no retardation introduced in Sec. IV under New. At the bottom are listed the rms deviation from experiment for each fit and the "best-fit" values of the parameters.

Meson	m_{expt}	BS	Th I	Th II	T	New
$\eta_c(1S)$	2979	3003	2989	3098	3150	3006
$\eta_c(2S)$	3595	3566	3563	3630	3635	3576
$\chi_{c0}(1P)$	3415	3356	3333	3402	3438	3330
$\chi_{c1}(1P)$	3511	3486	3477	3471	3495	3471
$h_c(1P)$	3526	3502	3500	3475	3498	3500
$J/\psi(1S)$	3097	3169	3151	3181	3225	3141
$\psi(2S)$	3686	3676	3668	3676	3674	3659
$\psi(3770)$	3770	3742	3741	3711	3715	3736
$\psi(4040)$	4040	4072	4088	4056	4004	4083
$\psi(4160)$	4159	4115	4135	4079	4031	4130
$\psi(4415)$	4415	4439	4491	4391	4293	4495
$\chi_{c2}(1P)$	3556	3624	3630	3583	3592	3634
$\chi_{b0}(1P)$	9860	9840	9861	9814	9803	9855
$\chi_{b0}(2P)$	10232	10183	10185	10182	10184	10191
$\chi_{b1}(1P)$	9892	9878	9912	9829	9818	9930
$\chi_{b1}(2P)$	10255	10218	10228	10193	10195	10243
$\Upsilon(1S)$	9460	9536	9531	9570	9551	9477
$\Upsilon(2S)$	10023	9998	10008	10000	9998	10017
$\Upsilon(3S)$	10355	10325	10318	10339	10346	10324
$\Upsilon(4S)$	10580	10599	10573	10631	10641	10568
$\Upsilon(10860)$	10865	10842	10800	10892	10902	10784
$\Upsilon(11020)$	11019	11065	11008	11131	11138	10981
$\chi_{b2}(1P)$	9913	9956	9995	9889	9881	10030
$\chi_{b2}(2P)$	10268	10284	10296	10248	10251	10318
rms	—	39	45	58	74	49
α_s	—	0.229	0.313	0.047	0.024	0.434
$\sigma(\text{GeV}^2)$	—	0.204	0.159	0.278	0.326	0.130
m_c (GeV)	—	1.28	1.37	1.14	1.16	1.46
m_b (GeV)	—	4.68	4.78	4.50	4.46	4.88

The parameter values (strong coupling, string tension, and quark masses) produced by the fits may also be compared with results of other model fits. For example Ref. [27] (the Particle Data Tables) lists what it calls "conservative" estimates for charm and bottom quark masses based on potential models. Because these mass estimates are from potential models, there is some logic in comparing them to the constituent quark masses produced by the QPE fits. Reference [27] lists the charm quark mass as 1.3–1.7 GeV and the bottom quark mass as 4.7–5.3 GeV. As Table IV shows, the two QPE's that gave the best fits in terms of rms deviation, the Thompson I and new equation, yielded both charm and bottom quark masses in accord with the ranges given by Ref. [27], though the Blankenbecler-Sugar equation's bottom mass prediction is only very slightly out of alignment with the Particle Data Table figures. We also note that the two equations having the worst rms deviations (the Thompson II and Todorov equations) produced best-fit strong couplings that seem unphysically low for the energy scales associated with charmonium and bottomonium.

Finally, we may compare the string tensions produced by each of the QPE fits with previous model fits and with expectations from lattice computations. Compilations of potential model results list string tensions generally falling in the range 0.18–0.2 GeV^2, e.g., [5,28]. Reference [5] lists the lattice computation estimates of string tension as $0.33^{+0.82}_{-0.23}$ GeV^2. Although each of the QPE's yielded best-fit values for string tension within the large limits supplied by this estimate, the $a \geq 0$ equations (Blankenbecler-Sugar, Thompson I, and new equations) produced numbers more in line with previous potential model work.

The purpose of the above fits to the heavy mesons was to test the qualitative intermediate coupling behavior of the Coulombic interaction in the equations being used to perform the fits. Fits based on minimizing the rms deviation from experiment were sufficient for this purpose. Therefore, no attempt was made to optimize a χ^2 fit by, for example, adjusting the parameters a and c of the generalized QPE or by trying more than two different Lorentz structures for the phenomenological linear confining potential. Nevertheless, it is interesting to compare the quality of these fits with others that have been reported.

Reference [29] presents χ^2 fits to 53 observed mesons including light, open-flavor, and heavy mesons using two-body Dirac equations. Of the 53 states, 23 were charmonium and bottomonium. The rms deviations for these heavy states were 23 MeV when using a vacuum-modified Richarson potential (RVP), 31 MeV when using an Adler-Peran potential (APP), and 46 MeV when using an unmodified Richardson model (RP). The Richardson potentials contained one parameter, and the Adler-Peran

potential two. The quality of these fits is especially noteworthy given the large number of meson states included in the fit.

Reference [10] lists results of fits to mesons composed of spinor quarks using Salpeter's equations and a form of the Blankenbecler-Sugar equation, all in momentum space. Scalar, scalar-plus-pseudoscalar, scalar-minus-pseudoscalar, and scalar-plus-vector Lorentz structures for the linear confinement potential were considered. Versions of Salpeter's equations which include coupling between positive and negative frequency states were used. A Breit interaction of the form

$$\Lambda_a^+\Lambda_b^+ V_{Br}\Lambda_a^+\Lambda_b^+ + \Lambda_a^-\Lambda_b^- V_{Br}\Lambda_a^-\Lambda_b^- \ , \qquad (22)$$

where

$$V_{Br} \sim \frac{\alpha_{\mathbf{a}}\cdot(\mathbf{p}-\mathbf{p}')\alpha_{\mathbf{b}}\cdot(\mathbf{p}-\mathbf{p}')}{(\mathbf{p}-\mathbf{p}')^4} \qquad (23)$$

was used in addition to interactions of the forms given in Eqs. (19) and (20) above. The best rms deviation for charmonium and bottomonium spectra fits was 42 MeV. These fits were performed by adjusting the same four quantities used in the fits of the present investigation.

Long [8] has produced a heavy meson spectrum also using spinor Salpeter's equations with coupling to negative energy components. Though no attempt was made to optimize the fit, Long reports an average difference of 36 MeV between experiment and calculation for 21 charmonium and bottomonium states.

We now use the Thompson I equation and the $a = 1$, $c = 0$ new equation, both with a scalar linear confining potential and OGE potential, to predict masses for those charmonium and bottomonium states which have not yet been measured experimentally (those states indicated by an asterisk in Table III). For both equations, we use the "best-fit" values for the quark masses, gluon coupling, and string tension as listed in Table IV. The predictions of the two equations are given in Table VI. The rms deviation between the predictions of these two models is 31 MeV for the 12 states, comparable to the rms deviations from experiment produced by these two equations when fitting the experimentally known states.

TABLE VI. Mass predictions using the Thompson I and New equations for those charmonium and bottomonium states not yet measured experimentally (indicated by asterisks in Table III). All masses are in MeV.

Meson	Th I	New
$\psi(4S)$	4345	4377
$\psi(5S)$	4593	4642
$\psi(6S)$	4811	4880
$\chi_{c0}(2P)$	3847	3859
$\chi_{c1}(2P)$	3906	3904
$\chi_{c2}(2P)$	3955	3985
$\eta_b(1S)$	9297	9338
$\eta_b(2S)$	9927	9950
$h_b(1P)$	9889	9892
$\Upsilon_b(1D)$	10131	10134
$\Upsilon_b(2D)$	10428	10426
$\Upsilon_b(3D)$	10683	10678

VI. FITS TO THE LIGHT MESONS

We extend the above treatment to the lighter mesons having up, down, and strange valence quarks. In this case, however, the justification for using only the valence quarks in a two-body potential formalism such as the QPE's to describe the mesons is not as well founded. Another difficulty is that it is questionable whether the valence structure of some of the light mesons is $q\bar{q}$. For example, Ref. [27] cites evidence that the $a_0(980)$ and $f_0(975)$ mesons are possibly non-$q\bar{q}$ in nature.

Our approach to the light meson spectroscopy is to assume flavor independence of the confining interaction and to fit the constituent quark masses (with $m_u = m_d$) and the gluon coupling constant. We selected ten light mesons for the fit and employed the Thompson I equation using the best value of the string tension of 0.212 GeV^2 from the heavy meson fit. We present the results in Table VII where the second column gives the spectral assignment used for each meson in the fit. These assignments are less certain than those for the heavy mesons. The fits were performed by minimizing the percent difference between each calculated energy and the corresponding experimentally measured mass. This strategy forces a better fit to the pion at the expense of degrading the rms deviations for the other nine mesons.

The rms deviation of this fit is 124 MeV. This may also be compared with the results reported in Refs. [29] and [10]. In the same χ^2 fit that produced the heavy meson results reported in the previous section, Ref. [29] obtained fits to nine light mesons with rms deviations of 65 MeV using RVP, 177 MeV using APP, and 87 MeV using RP. Reference [10], again using positive and negative frequency coupled Salpeter's equations, reports a fit to 13 light $q\bar{q}$ states with a rms deviation of 159 MeV.

Our approach has been to present reasonable fits with these QPE's rather than to carefully search for the best possible fits by, for example, allowing mixtures of other Lorentz structures in the confinement potential. The

TABLE VII. Thompson I QPE fit to ten light quark mesons. All masses are in MeV. At the bottom are listed the rms deviations from experiment and the best-fit values of parameters. The string tension was 0.212 GeV^2 from the heavy meson fit.

Meson	$N\,^{2S+1}L_J$	m_{expt}	Th I
$\pi^{\pm}$	$1\,^1S_0$	140	139
$\pi(1300)$	$2\,^1S_0$	1300	1053
$\pi_2(1670)$	$1\,^1D_2$	1670	1460
$a_1(1260)$	$1\,^3P_1$	1260	1201
$b_1(1235)$	$1\,^1P_1$	1232	1214
$\rho(770)$	$1\,^3S_1$	768	926
$a_2(1320)$	$1\,^3P_2$	1318	1348
$\phi(1020)$	$1\,^3S_1$	1019	1067
$\phi'(1680)$	$2\,^3S_1$	1680	1577
f_2'	$1\,^3P_2$	1525	1516
rms deviation	—	—	124
α_s	—	—	0.52
m_u	—	—	334
m_s	—	—	407

qualitative results for the light mesons which emerge are encouraging in that the constituent quark masses are in line with other models and the gluon coupling is about 60% stronger than the Thompson I fit to the heavy mesons. It is also interesting to note that the α_s obtained in the light meson fit is close to the assumed saturation value of α_s employed in Ref. [3].

VII. DEEP BINDING LIMIT

Several studies have been performed recently on the large coupling (deep binding) regime of bound state systems. Some of these investigations have been done in the context of bound states of very massive fermions where the binding effect of Higgs boson exchange is very large [30]. Others have been concerned with the attempt to bootstrap the Higgs boson (e.g., Ref. [31]). The equations that have been used as approximations to the full BSE in these studies have the property that they drive the total energy of the two-particle bound state to zero as the coupling strength of the binding interaction is increased.

Some authors interpret the vanishing meson mass as unphysical and they construct some relativistic equations which do not drive the bound state mass to zero at large coupling, e.g., Ref. [32]. Here we note that any ladder QPE arising from use of the generalized propagator in which $a > 0$ will not produce zero energy bound states at large coupling. As Eq. (14) shows, such a propagator will have a powers of the energy in the numerator. A solution with the bound state mass equal to zero would make the propagator vanish, and the QPE would then have no nontrivial solution.

As an example of the large coupling behavior of such a QPE, we display in Fig. 2 the total energy predicted by the fermion-antifermion QPE with $a = 1$ and $c = 0$ introduced in Sec. IV for couplings in the range 0–5. We also present for comparison the fourth order perturbative energies plotted against coupling strength. At small coupling, the energy predicted by the QPE is indistinguishable from the perturbative result on the scale of the plot. The perturbative result drives the total energy to zero before the coupling reaches 1.5. However, the QPE has no nontrivial solution for zero energy. Though it predicts increased binding as the coupling increases, the energy is still well above zero even when the coupling is as large as 5.

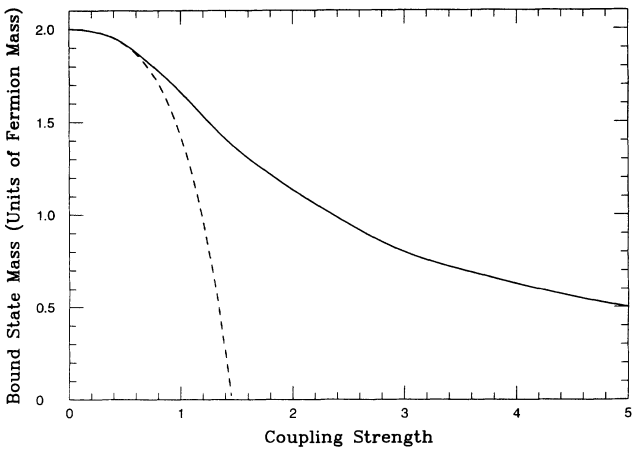

FIG. 2. The bound state mass predicted by $a = 1$, $c = 0$ new QPE (with no retardation) of Sec. IV (solid curve) and by fourth order perturbation theory (dashed curve) as a function of coupling strength λ. At small coupling the curves are indistinguishable. At large coupling the perturbative solution drives the bound state mass to zero while the QPE solution remains positive.

VIII. SUMMARY AND OUTLOOK

We have performed an examination of the feasibility of using the quasipotential equation formalism as a tool for studying hadronic physics. The equations we investigated are covariant, employ a full nonlocal one-gluon-exchange potential, and a linear confining interaction motivated by lattice QCD calculations. We have used no explicit regulators in our equations, thus minimizing the number of parameters, and we have identified a class of QPE's that provide a good fit to the quarkonia spectra (32–36 MeV rms deviation from experiment for the best heavy meson fits) with reasonable potential parameters. A somewhat lesser quality fit is obtained for the light mesons, but the rms deviation between model and experiment is reasonably competitive with other relativistic formalisms.

Much more stringent tests of the various two-body equations are provided by calculations of other observables such as decay constants and form factors. The results and analyses of the present paper demonstrate that the covariant QPE's can be a powerful means of investigating strong coupling physics. With this preliminary investigation completed, the stage is set for the introduction of further physics (running couplings, annihilation graphs, etc.) into the integral equations. Among our goals are to complete an improved description of the light and open-flavor mesons, calculate a complete set of decay constants and widths, and investigate in-medium effects of meson observables.

ACKNOWLEDGMENTS

This work was supported in part by the U.S. Department of Energy under Grant No. DE-FG02-87ER40371, Division of High Energy and Nuclear Physics. We appreciate the hospitality of the Institute for Nuclear Theory in Seattle, Washington where a portion of this work was conducted. One of us (J.P.V.) acknowledges support of the Alexander von Humboldt Foundation.

APPENDIX: BRIEF OUTLINE OF THE METHOD OF SOLUTION

The methods we employ for solving the QPE's have been described elsewhere ([8,10] and particularly [26] and references therein), and the full details will not be re-

peated here. In this appendix we provide an overview of the method.

A standard partial wave reduction in a basis of total angular momentum states is performed on the integrand of the wave equation:

$$\sum_L \int dp' p'^2 \langle JML'S|V(\mathbf{p},\mathbf{p}')|JMLS\rangle\langle JMLS|\psi(p')\rangle, \tag{A1}$$

where $L = L' = J$ or $L = L' = J \pm 1$ depending on which angular momentum channel is being solved. Integrals such as

$$\int d\Omega'(\mathbf{p}-\mathbf{p}')^{-2} P_J(\theta') = \frac{2\pi}{pp'} Q_J(Z), \tag{A2}$$

where the $P_J(\theta)$ are the Legendre polynomials and the $Q_J(Z)$ are the Legendre functions of the second kind with argument $Z = (p^2 + p'^2)/2pp'$, are used to express the matrix elements of $V_{\rm OGE}$ in the form

$$\langle JML'S|V(\mathbf{p},\mathbf{p}')|JMLS\rangle = \sum_k A^k_{JMLL'S} Q_k(Z). \tag{A3}$$

The Legendre functions of the second kind have the form

$$Q_0(Z) = \tfrac{1}{2}\ln\left[\frac{Z+1}{Z-1}\right], \tag{A4a}$$

with the recursion relation

$$Q_{J+1}(Z) = \left[\frac{2J+1}{J+1}\right] Z Q_J(Z) - \frac{J}{J+1} Q_{j-1}(Z) - \delta_{J,0}. \tag{A4b}$$

Similarly, the form of $V_{\rm con}$ given in Eq. (20) results in matrix elements of the form

$$\langle JML'S|V(\mathbf{p},\mathbf{p}')|JMLS\rangle$$

$$= \lim_{\mu\to 0}\left(\frac{\partial}{\partial\mu}\right)^2 \sum_k B^k_{JMLL'S} Q_k(Z') \tag{A5}$$

where now $Z' = (p^2 + p'^2 + \mu^2)/2pp'$.

The partial wave amplitudes are expressed as a sum of cubic basis splines (B splines) $B_\nu(p)$,

$$\langle JMLS|\psi(p)\rangle \simeq \sum_{\nu=1}^{N} a_\nu B_\nu(p). \tag{A6}$$

Each of the B splines is constructed from cubic polynomials in momentum space. Each polynomial is defined over an interval in momentum space bounded by points called knots. Each B spline is nonzero over four adjacent such intervals. Such a span defined by four adjacent intervals involves five knots. The B spline is constructed by joining the four cubic polynomials for these four intervals at the three middle knots in such a way that their first two derivatives are equal at the knots. At the first and last knots, the B spline is constructed to have a value of zero with vanishing first and second derivatives. The finite span of the momentum space axis to be used in solving the equation is divided into a series of intervals defined by $N+4$ knots, and this span is then covered by N distinct B splines.

In the integrand there will be functions of p and p', which we may call $F(p,p')$, arising from the partial wave reductions of the interactions and from the quasipotential propagators. The specific form that F takes will vary depending on which QPE is being solved. A second ingredient in the solution method is to approximate $F(p,p')$ by a cubic polynomial on each B-spline knot interval. That is, on each knot interval we have

$$F(p,p') \simeq \sum_{n=0}^{3} c_n(p) p'^n. \tag{A7}$$

By then operating on the entire equation from the left with $\int dp B_\mu(p)$, an equation results which has the form

$$E\sum_\nu \int dp B_\mu(p) B_\nu(p) a_\nu$$

$$= \sum_\nu \int dp B_\mu(p) T B_\nu(p) a_\nu + \sum_\nu \int dp B_\mu(p) \int dp' I(p,p') B_\nu(p') a_\nu. \tag{A8}$$

Here, E is the eigenvalue, T is relativistic kinetic energy operator, and $I(p,p')$ is the polynomial representation of $F(p,p')$ from Eq. (A7) multiplied by linear combinations of the $Q_k(Z)$. Since $I(p,p')$ consists of only polynomials and logarithms, the p' integration in Eq. (A8) may be done analytically. It is important that such an integral over the logarithms in the Legendre functions be done analytically since numerical integration over the logarithmic singularities in $Q_k(Z)$ would be very unstabe. The remaining p integration in Eq. (A8) is done numerically. Equation (A8) may be expressed as a matrix equation

$$E B_{\mu\nu} a_\nu = (T_{\mu\nu} + V_{\mu\nu}) a_\nu, \tag{A9}$$

where the banded-diagonal metric $B_{\mu\nu}$ appears because of the nonorthogonal spline basis functions. Equation (A9) is solved for the eigenvalue E and eigenvector a_ν with standard matrix equation techniques.

[1] For reviews of the field see J. B. Kogut, Phys. Rep. **67**, 67 (1980); C. Rebbi, *ibid.* **137**, 63 (1986).
[2] E. Eichten, K. Gottfried, T. Kinoshita, R. D. Lane, and T. D. Yan, Phys. Rev. D **17**, 3090 (1978); **21**, 203 (1980).
[3] S. Godfrey and N. Isgur, Phys. Rev. D **32**, 189 (1985).
[4] S. Godfrey, Nuovo Cimento A **102**, 1 (1989).
[5] W. Lucha, F. F. Schöberl, and D. Gromes, Phys. Rep. **200**, 127 (1991).
[6] E. Laermann, in Proceedings of Particles and Nuclei International Conference XIII (World Scientific, Singapore, in press).
[7] E. E. Salpeter and H. A. Bethe, Phys. Rev. **84**, 1232 (1951).
[8] C. Long, Phys. Rev. D **30**, 1970 (1984); D. Eyre and J.

P. Vary, *ibid.* **34**, 3467 (1986); J. R. Spence and J. P. Vary, *ibid.* **35**, 2191 (1987).
[9] F. Gross and J. Milana, Phys. Rev. D **43**, 2401 (1991); **45**, 969 (1992); P. C. Tiemeijer and J. A. Tjon, Phys. Lett. B **277**, 38 (1992); K. M. Maung, D. E. Kahana, and J. W. Norbury, Phys. Rev. D **47**, 1182 (1993).
[10] J. R. Spence and J. P. Vary, Phys. Rev. C **47**, 1282 (1993).
[11] G. E. Brown and A. D. Jackson, *The Nucleon-Nucleon Interaction* (North-Holland, New York, 1976), Chap. 6.
[12] E. E. Salpeter, Phys. Rev. **87**, 328 (1952).
[13] R. J. Yaes, Phys. Rev. D **3**, 3086 (1971).
[14] R. Blankenbecler and R. Sugar, Phys. Rev. **142**, 1051 (1966).
[15] V. G. Kadyshevsky, Nucl. Phys. **B6**, 125 (1968).
[16] F. Gross, Phys. Rev. **186**, 1448 (1969).
[17] R. H. Thompson, Phys. Rev. D **1**, 110 (1970).
[18] I. T. Todorov, Phys. Rev. D **3**, 2351 (1971).
[19] K. Erkelenz and K. Holinde, Nucl. Phys. **A194**, 161 (1972).
[20] R. M. Woloshyn and A. D. Jackson, Nucl. Phys. **B64**, 269 (1973).
[21] F. Gross, Phys. Rev. C **26**, 2203 (1982).
[22] B. Silvestre-Brac, A. Bilial, C. Gignoux, and P. Schuck, Phys. Rev. D **29**, 2275 (1984).
[23] E. D. Cooper and B. K. Jennings, Nucl. Phys. **A483**, 601 (1988).
[24] C. Itzykson and I. Zuber, *Quantum Field Theory* (McGraw-Hill, New York, 1980), Sec. 10-3-2.
[25] H. A. Bethe and E. E. Salpeter, *Quantum Mechanics of One- and Two-Electron Atoms* (Plenum, New York, 1977), Sec. 23.
[26] C. de Boor, *A Practical Guide to Splines* (Springer-Verlag, New York, 1978); M. Brannigan and D. Eyre, J. Math Phys. **24**, 1548 (1983).
[27] Particle Data Group, Phys. Rev. D **45**, Sec. VII (1992).
[28] W. Kwong, J. L. Rosner, and C. Quigg, Annu. Rev. Nucl. Part. Sci. **37**, 325 (1987).
[29] H. W. Crater and P. Van Alstine, Phys. Rev. D **37**, 1982 (1988).
[30] P. Jain, A. J. Sommerer, D. W. McKay, J. R. Spence, J. P. Vary, and B.-L. Young, Phys. Rev. D **46**, 4029 (1992).
[31] G. Rupp, Phys. Lett. B **288**, 99 (1992).
[32] H. W. Crater, Phys. Rev. D **12**, 1804 (1975).